

# Template-assisted Preparation of Self-standing 2D-MOF Membranes for Application in Cascade Reactions

Yingying Du,<sup>[a]</sup> Chenhui Ding,<sup>[a]</sup> Jana Timm,<sup>[b]</sup> Roland Marschall,<sup>[b]</sup> and Seema Agarwal\*<sup>[a]</sup>

Self-standing metal-organic framework (MOF) membranes open up several application areas where their use in the powder form is either not possible or non-sustainable. Most MOF membranes are prepared as a thin layer either on a supporting substrate or used as a composite membrane with additional supporting material. In this work, we present the preparation procedure for making highly stable, easy-to-handle, reusable, efficient pure MOF membranes (UiO-66-SO<sub>3</sub>H and UiO-66-NH<sub>2</sub> membranes; thickness 240 ± 12 μm and 265 ± 10 μm, respectively) with hollow fiber morphology and their use in cascade reactions in

one-pot catalyzed by incompatible acid-base in tea-bag-type concept. The catalytic performance of the catalyst membranes was tested by reacting benzaldehyde dimethyl acetal with three active methylene compounds. The membranes exhibited excellent catalytic activity in cascade reactions in one pot (the yield of the product was as high as 99.9%) and can be reutilized up to 15 times without any significant loss in activity. Stable pure MOF membranes, as shown in this work, would be of interest for several other applications beyond catalysis.

## Introduction

Metal-organic frameworks (MOFs) with large surface area, tunable pore size, porosities, and high thermal and chemical stability emerged as important porous materials for several applications, such as gas separation, oil-water separation, etc.<sup>[1]</sup> MOFs are framework structures formed by the self-assembly of metal clusters and organic ligands through coordination bonds as an insoluble and post-synthesis non-processable powder.<sup>[2]</sup> MOF was grown on a substrate using an in-situ growth method to enable their use in several application areas where a film is required. One of the methods utilizes immersion of an inorganic substrate in a MOF reaction solution.<sup>[3]</sup> Further improvement is made by modifying the inorganic surface that provides nucleation sites for MOF's growth and improves the substrate-MOF adhesion.<sup>[4]</sup> Other methods using already prepared MOF nanoparticles (e.g., ZIF-8) as seeds for the growth of thin MOF film on an inorganic or polymer substrate are also studied.<sup>[5]</sup>

The use of MOF in heterogenous catalysis in one-pot cascade reactions is recently getting more and more attention as a sustainable alternative to multi-step reactions.<sup>[6]</sup> The intermediate processing steps, such as the removal and

purification of products at each stage, are eliminated in one-pot cascade reactions, simplifying the synthetic procedure, reducing the solvents' use, and minimizing waste generation.<sup>[7]</sup> Besides MOF, several examples of cascade reactions using different catalysts (homogenous, enzymes, and heterogenous) for an individual sequence of reactions in a cascade are also known.<sup>[8]</sup>

One-pot cascade reactions with catalysts that deactivate each other are more challenging as they require carefully designed catalyst support architectures that keep the individual catalysts isolated from each other in an active state.<sup>[9]</sup> The incompatible catalysts which deactivate each other on coming into contact are called Wolf-Lamb-type catalysts. Moreover, easy and complete recovery after the reaction is of utmost importance for the sustainable use of catalysts. The recovered catalysts can be reused in several other catalytic reactions without losing activity. This makes the design of catalyst support architecture furthermore challenging.

Several efforts are invested in providing solutions to this challenge, and different catalytic supports keeping the two or more incompatible active catalysts isolated from each other in one pot are reported in the literature. For this, polymer resins and magnetic nanoparticles,<sup>[10]</sup> acidic- and basic-layered silicates,<sup>[11]</sup> zeolites,<sup>[12]</sup> and metal-organic frameworks (MOFs)<sup>[13]</sup> are highlighted.


MOFs as catalyst support has increased in the last years due to high porosity, specific surface area, and possibilities of tuning their structure.<sup>[14]</sup> In particular, acid-base bifunctional MOF powder is an effective catalyst for cascade reactions in one pot.<sup>[15]</sup> Complex catalyst supports, such as egg yolk-shell structured covalent organic framework (COF)@MOF (YS-COF@MOF), were also used for the site-separation of acidic and basic groups.<sup>[16]</sup> MOF is prepared and subsequently used mostly in the form of nanoparticles, which can agglomerate during reactions. Also, retrieving MOF nanoparticles requires an additional filtration or magnetic separation step.<sup>[17]</sup> Future efforts are


[a] Y. Du, C. Ding, S. Agarwal

Macromolecular Chemistry and Bavarian Polymer Institute  
University of Bayreuth  
Universitätsstrasse 30, 95440 Bayreuth (Germany)  
E-mail: agarwal@uni-bayreuth.de

[b] J. Timm, R. Marschall

Department of Chemistry  
Physical Chemistry III  
University of Bayreuth  
Universitätsstrasse 30, 95440 Bayreuth (Germany)

 Supporting information for this article is available on the WWW under <https://doi.org/10.1002/cctc.202201040>

 © 2022 The Authors. ChemCatChem published by Wiley-VCH GmbH. This is an open access article under the terms of the Creative Commons Attribution License, which permits use, distribution and reproduction in any medium, provided the original work is properly cited.

needed to design efficient incompatible catalyst supports that are easily reusable.

Previously, we reported a teabag-type concept for reusable heterogeneous catalysis in which catalysts can be removed easily, like a teabag from tea, and reused. For example, gold nanoparticles (AuNPs) were incorporated in high surface-to-volume hollow polymer fibers, forming a porous nonwoven membrane by randomly laying these fibers by electrospinning. It catalyzed the hydrolytic oxidation of dimethyl phenyl silane and the alcoholysis of dimethyl phenyl silane with *n*-butanol. The catalytic non-woven was taken out for reuse in the same way as a teabag after use.<sup>[18]</sup> Keeping our focus on the tea-bag-type concept for catalysts' reusability, we later prepared catalytic supports for incompatible acid and base catalysts. We electrospun and later cross-linked the fibers in nonwoven prepared from  $-SO_3H$  and  $-NH_2$  functional polymers and used them in one-pot cascade reactions: deacetylation and subsequent reaction of an aldehyde with reactive methylene compounds.<sup>[19]</sup> Efficient catalysis was observed, but the soft polymer catalyst membranes were easily swollen by the solvents used for reactions to form a gel, reducing the catalyst's service life.

In this work, we present a preparation procedure for making highly stable, easy-to-handle, reusable, efficient self-standing pure MOF membranes based on well-known MOF (UiO-66)<sup>[20]</sup> for use in acid-base catalyzed cascade reactions in one-pot in tea-bag-type concept. After use, the catalyst membranes can be simply removed, washed, and reused for the next cycles of reactions. A procedure for making such self-standing MOF membranes with functional groups  $-SO_3H$  and  $-NH_2$  is described, followed by detailed studies regarding their catalytic ability in cascade reactions in one pot. The catalyst membranes exhibited excellent catalytic activity in the acid-base catalyzed reactions (the yield was as high as 99.9%). Moreover, it reveals the same activity on reusing at least 15 catalytic cycles. The details of the material preparation and use in one-pot acid-base

catalyzed reactions are described in detail in the results and discussion section.

## Results and discussion

The synthesis strategy of making MOF (UiO-66- $SO_3H$ ) (acid-functionalized) and MOF (UiO-66- $NH_2$ ) (base-functionalized) individual porous membranes is shown in Figure 1. First, a fiber membrane of polyacrylonitrile (PAN) as a template polymer, together with  $ZrCl_4$ , was obtained by electrospinning a mixed solution of  $ZrCl_4$  and PAN in DMF. The optical photographs of the PAN/ $ZrCl_4$  membrane are shown in Figure S1. The membrane was obtained as a non-woven by random deposition of fibers (average diameter 500 nm and thickness  $78 \pm 10 \mu m$ ) (Figure S1). Next, using the in-situ growth method, MOF (UiO-66- $SO_3H$  and UiO-66- $NH_2$ ) were grown on PAN membrane using the acetic acid catalyst in the water together with either 2-aminobenzenedicarboxylic acid (BDC- $NH_2$ ) or 2-sulfobenzenedicarboxylic acid monosodium salt (BDC- $SO_3Na$ ). In the next step, the template polymer, PAN was removed by Soxhlet extraction with DMF leaves behind UiO-66- $SO_3H$  and UiO-66- $NH_2$  membranes of thickness  $240 \pm 12 \mu m$  and  $265 \pm 10 \mu m$ , respectively.

A scanning electron microscope (SEM) was used to characterize the morphology of the synthesized UiO-66- $SO_3H$ / $-NH_2$  membranes before and after PAN removal, as shown in Figure 2. Figures 2a, and 2b are PAN/UiO-66- $SO_3H$  and PAN/UiO-66- $NH_2$  membranes, respectively. Through the in-situ growth, a large amount of MOF grows on the surface of PAN fiber and completely wraps them. Figure 2c, and 2d are the surface morphologies of the UiO-66- $SO_3H$  membrane and UiO-66- $NH_2$  membrane observed under SEM after removing the template polymer PAN by Soxhlet extraction. After removing PAN, the membrane remained intact. Figure 2e, and 2f are the cross-sectional images of UiO-66- $SO_3H$  and UiO-66- $NH_2$  membranes, respectively, after the removal of PAN, which shows

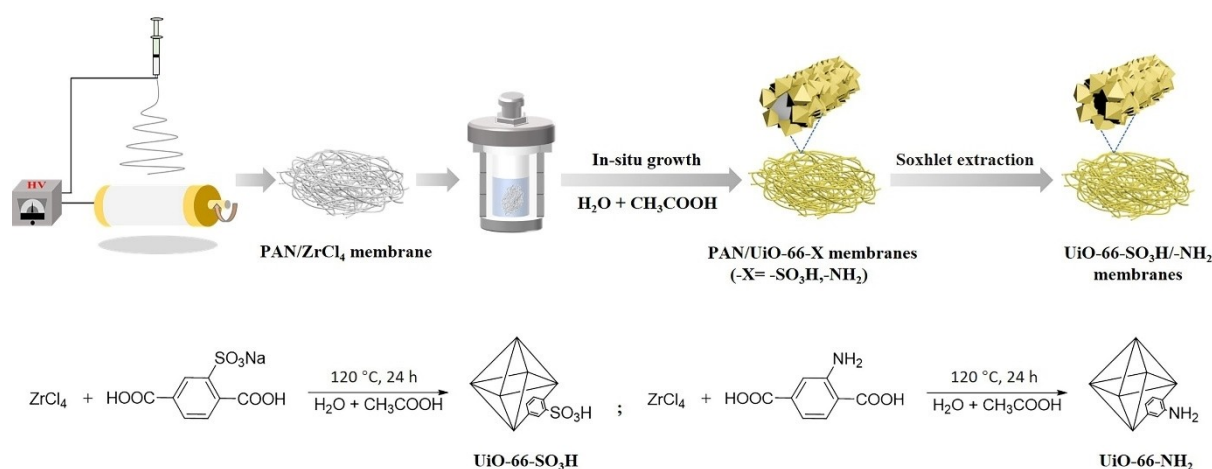


**Figure 1.** Strategy to fabricate the self-standing UiO-66- $SO_3H$  and UiO-66- $NH_2$  membranes (top) and the reaction scheme to prepare corresponding MOFs (bottom).

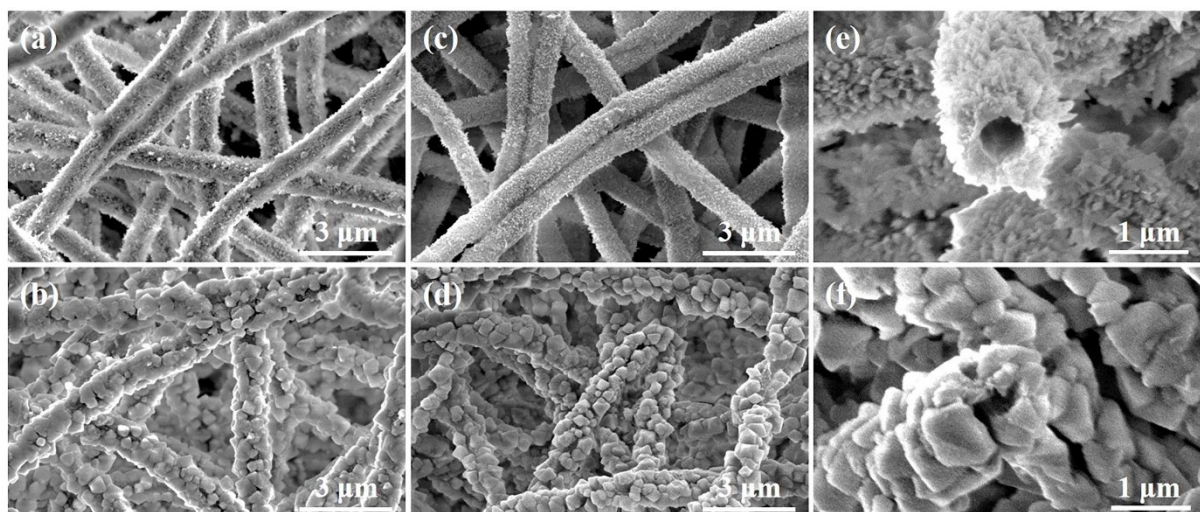


**Figure 2.** SEM morphology of a) PAN/UiO-66-SO<sub>3</sub>H, b) PAN/UiO-66-NH<sub>2</sub>, c) UiO-66-SO<sub>3</sub>H, d) UiO-66-NH<sub>2</sub>, Cross-sectional SEM morphology of e) UiO-66-SO<sub>3</sub>H, f) UiO-66-NH<sub>2</sub> membranes.

hollow MOF fibers. The optical photographs of UiO-66-SO<sub>3</sub>H and UiO-66-NH<sub>2</sub> membranes are shown in Figure S1.

The distinct peaks at  $2\theta = 7.52^\circ$ ,  $8.69^\circ$  and the absence of a peak at  $2\theta = 17.07^\circ$  originating from the template polymer

(PAN) (Figure 3a) in XRD confirmed the preparation of UiO-66-SO<sub>3</sub>H/-NH<sub>2</sub> membranes.<sup>[21]</sup> Compared with MOF powder, the characteristic peaks of MOF membranes are broader. But the main characteristic peak still exists, indicating that Soxhlet

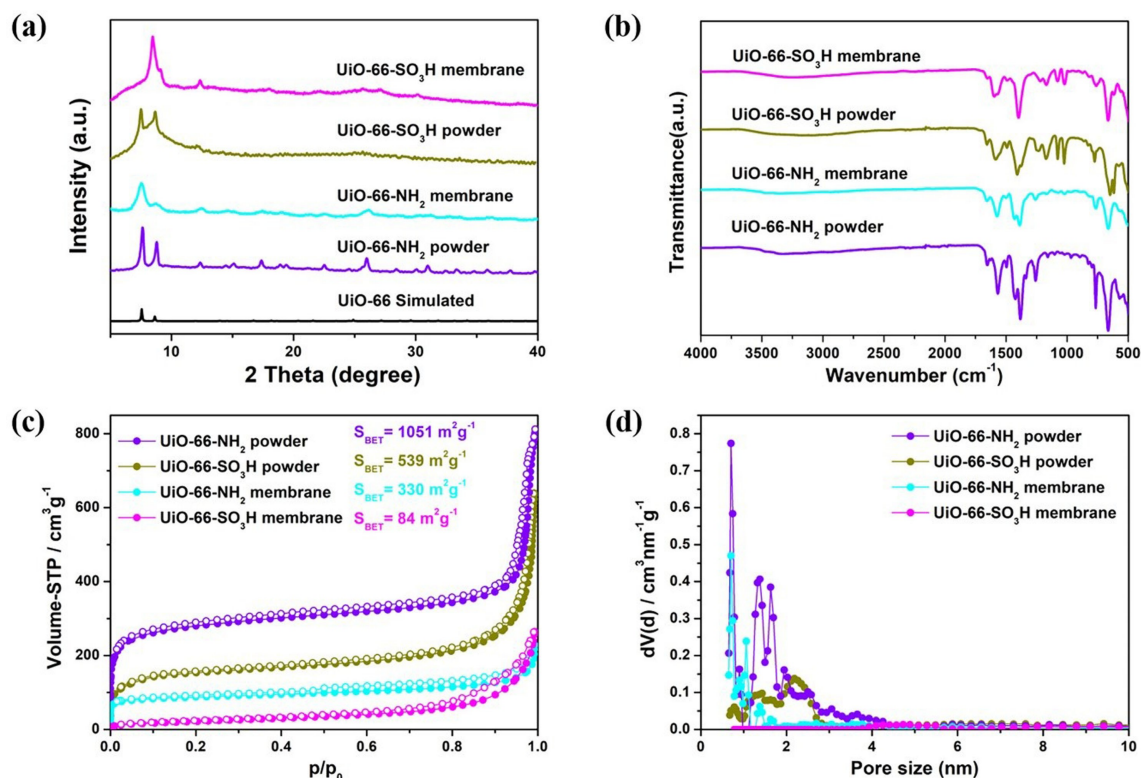


**Figure 3.** a) XRD patterns of UiO-66 simulated, UiO-66-SO<sub>3</sub>H powder, UiO-66-SO<sub>3</sub>H membrane, UiO-66-NH<sub>2</sub> powder and UiO-66-NH<sub>2</sub> membrane. b) FT-IR spectra of UiO-66-SO<sub>3</sub>H powder, UiO-66-SO<sub>3</sub>H membrane, UiO-66-NH<sub>2</sub> powder and UiO-66-NH<sub>2</sub> membrane. c) N<sub>2</sub> physisorption isotherms of UiO-66-SO<sub>3</sub>H powder, UiO-66-SO<sub>3</sub>H membrane, UiO-66-NH<sub>2</sub> powder and UiO-66-NH<sub>2</sub> membrane. d) Pore size distribution and cumulative pore volume of UiO-66-SO<sub>3</sub>H powder, UiO-66-SO<sub>3</sub>H membrane, UiO-66-NH<sub>2</sub> powder and UiO-66-NH<sub>2</sub> membrane.



extraction has caused a certain degree of disorder or inhomogeneity in crystallite size within the framework, but the overall phase integrity is preserved.<sup>[22]</sup>

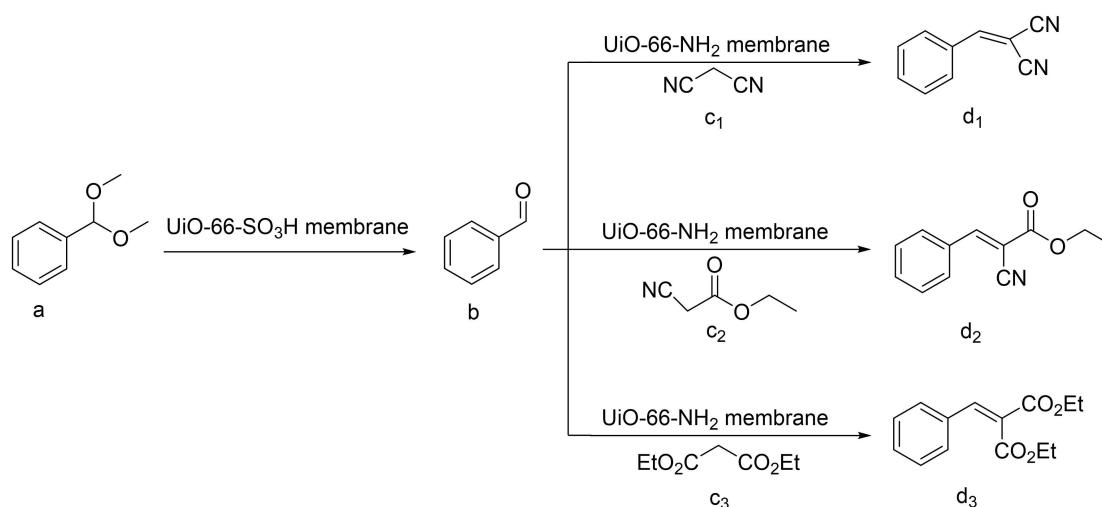
In the infrared spectrum of the UiO-66-SO<sub>3</sub>H membrane, the characteristic stretching bands at 1074 cm<sup>-1</sup> and 1024 cm<sup>-1</sup> are S–O, and at 1253 cm<sup>-1</sup> and 1167 cm<sup>-1</sup> from O=S=O could be observed (Figure 3b).<sup>[23]</sup> In the infrared spectrum of the UiO-66-NH<sub>2</sub> membrane, the appearance of an absorption band at 1572 cm<sup>-1</sup> indicates the reaction of -COOH with Zr<sup>4+</sup>. The 1502 cm<sup>-1</sup> band is from aromatic C=C.<sup>[15a]</sup> The main characteristic peak of polyacrylonitrile C≡N was seen at 2245 cm<sup>-1</sup>. By comparison, the self-standing UiO-66-SO<sub>3</sub>H and UiO-66-NH<sub>2</sub> membranes did not show the characteristic peak of C≡N at 2245 cm<sup>-1</sup> (Figure S2b). This confirms the successful preparation of independent self-standing UiO-66-SO<sub>3</sub>H/-NH<sub>2</sub> membranes.

N<sub>2</sub> physisorption isotherm provided pore size distribution and specific surface area of the powders and membranes, as shown in Figure 3. The Nitrogen physisorption isotherms of all samples indicate micropores in the materials due to a sharp increase at very low relative pressures (*p/p*<sub>0</sub>) (Figure 3c). Additionally, small mesopores were found in all materials (Figure 3d).<sup>[24]</sup> At *p/p*<sub>0</sub> > 0.5, the shape of the physisorption isotherms of the powders and the membranes are different. This change might be explained by the formation of the nanostructured fiber morphology and cavitation effects (effects not visible in the pore size distribution due to fitting the adsorption of the physisorption isotherm).<sup>[25]</sup> When comparing the pore size distributions (PSD) of the powders and the membranes, the similarity is very impressive and shows that even characteristics of MOFs (high porosity and well-defined pores) could be assigned to a membrane by the used synthetic approach. The specific surface areas of the membranes, as calculated using the BET (Brunauer Emmet Teller) model with the Roquerol correction for microporous materials<sup>[26]</sup> are significantly lower (UiO-66-NH<sub>2</sub>: 330 m<sup>2</sup>g<sup>-1</sup>, UiO-66-SO<sub>3</sub>H: 84 m<sup>2</sup>g<sup>-1</sup>) than the specific surface areas of powder samples (UiO-66-NH<sub>2</sub>: 1051 m<sup>2</sup>g<sup>-1</sup> UiO-66-SO<sub>3</sub>H: 539 m<sup>2</sup>g<sup>-1</sup>). This de-

crease in the surface area could be explained by the partial change in the crystal structure or surface tension of the crystals of the UiO-66 materials, which was already observed due to the broadening of the reflections in the XRD pattern (Figure 3a).

Further, the self-supporting MOFs were studied in one pot as acid-base catalysts for a sequence of two steps, as shown in Scheme 1 (for reaction mechanism, please refer to Scheme S1). Three different one-pot reactions were studied. In each of the three reactions, the UiO-66-SO<sub>3</sub>H membrane is intended to catalyze the conversion of benzaldehyde dimethyl acetal to benzaldehyde as the first step. At the same time, the UiO-66-NH<sub>2</sub> membrane is designed to catalyze the subsequent reaction of benzaldehyde with different active methylene compounds, such as malononitrile and ethyl cyanoacetate, and diethyl malonate. Benzaldehyde undergoes cyanation by malononitrile, whereas ethyl cyanoacetate and diethyl malonate undergo Knoevenagel condensation with benzaldehyde.

Before starting one-pot reactions, the acid and base-MOF membranes were tested for the individual reaction steps in different pots. The UiO-66-SO<sub>3</sub>H membrane catalyzed the deacetylation reaction, as shown in Scheme 1-step a to b and Figure S3a. The molar ratio of benzaldehyde dimethyl acetal to UiO-66-SO<sub>3</sub>H catalyst was 1:0.0233. The reaction was fast. About 85% of the theoretical amount of benzaldehyde was already obtained in 15 minutes. The conversion rate as determined from the initial portion of the % conversion vs. time curve (Figure S3a) till about 15 minutes was 5.69%·min<sup>-1</sup>. After this, although there was a slow down in the rate of reaction, still very high conversion (> 95% of benzaldehyde) was obtained in about 60 minutes (rate = 1.56%·min<sup>-1</sup>). The UiO-66-NH<sub>2</sub> membrane catalyzed the reaction of benzaldehyde and malononitrile, as shown in Figure S3b. The molar ratio of benzaldehyde to UiO-66-NH<sub>2</sub> catalyst was 1:0.0565. Approximately after 30 minutes, 80% of benzaldehyde was converted to 2-benzylidene malononitrile (rate = 2.49%·min<sup>-1</sup>). The benzaldehyde was almost completely converted into 2-benzylidene malononitrile when the reaction proceeded for 120 minutes.



**Scheme 1.** Wolf-Lamb-type one-pot cascade reactions were studied in the present work.

The one-pot, two-step catalysis experiment results are shown in Figure 4a. For one-pot two steps reactions, both The UiO-66-NH<sub>2</sub> and UiO-66-SO<sub>3</sub>H membranes were inserted in a reaction vessel, and all reagents were added simultaneously. Benzaldehyde dimethyl acetal (0.0025 mol), UiO-66-SO<sub>3</sub>H catalyst (0.58 × 10<sup>-4</sup> mol) and UiO-66-NH<sub>2</sub> catalyst (1.4 × 10<sup>-4</sup> mol) were used for the reaction. The reaction was monitored for the formation of products by gas chromatography (GC). After 30 minutes, more than 80% of benzaldehyde dimethyl acetal was consumed (rate = 2.81% · min<sup>-1</sup>). After a small induction period, the final product 2-benzylidene malononitrile started forming with a ~1.11% min<sup>-1</sup> conversion rate until about 60 minutes. After this, although the production rate of 2-benzylidene malononitrile decreased (1.06% · min<sup>-1</sup>), the reaction was still completed until very high conversions (99.9% in 4 h).

Since the first step, the UiO-66-SO<sub>3</sub>H membrane catalyzed reaction, is the same, we only studied the base UiO-66-NH<sub>2</sub> catalyzed conversion of benzaldehyde in the next set of reactions to ethyl-2-cyano-3-phenyl acrylate, as shown in Figure S3c. No inhibition time was found. 70% of the benzaldehyde was converted into the product ethyl-2-cyano-3-phenyl acrylate after only 90 minutes (rate = 0.78% · min<sup>-1</sup>), and about 95% conversion to the product was achieved after 7 hours of reaction. Afterward, acid UiO-66-SO<sub>3</sub>H and base UiO-66-NH<sub>2</sub> membranes were used together to study the kinetics of acid-

base-catalyzed two-step reactions in one pot. The results of the one-pot, two-step reaction of the production of benzaldehyde from benzaldehyde dimethyl acetal and its further reaction with ethyl cyanoacetate are shown in Figure 4b. The results were very promising. After a slow start, the rate of reaction increased. About 88% of the product was achieved in 7 h (rate = 12.6% · h<sup>-1</sup>) with almost quantitative conversion in 8 h.

Encouraged by the above results, we tested the reaction of benzaldehyde dimethyl acetal with diethyl malonate. The base UiO-66-NH<sub>2</sub> catalyzed the conversion of benzaldehyde to diethyl 2-benzylidene malonate, as shown in Figure S3d.

Unfortunately, the reaction proceeded very slowly, with only 37% of diethyl 2-benzylidene malonate produced (rate = 3.21% · h<sup>-1</sup>). The results of the one-pot, two-step reaction of the production of benzaldehyde from benzaldehyde dimethyl acetal and its further reaction with diethyl malonate are shown in Figure 4c. The dimethoxybenzyl acetal was only 74% converted in this reaction, and at the end of the reaction, only 36.7% of the product was produced (rate = 2.42% · h<sup>-1</sup>). We speculate that this may be because the pK<sub>a</sub> value of diethyl malonate is too high. Malononitrile (pK<sub>a</sub> = 11.1), ethyl cyanoacetate (pK<sub>a</sub> = 13.2), diethyl malonate (pK<sub>a</sub> = 16.3).<sup>[27]</sup> Due to the high pK<sub>a</sub> of diethyl malonate, deprotonation of methylene groups is extremely difficult, resulting in low product yields in one-pot reactions. There have been similar reports of this phenomenon before.<sup>[28]</sup> In addition, we investigated blank

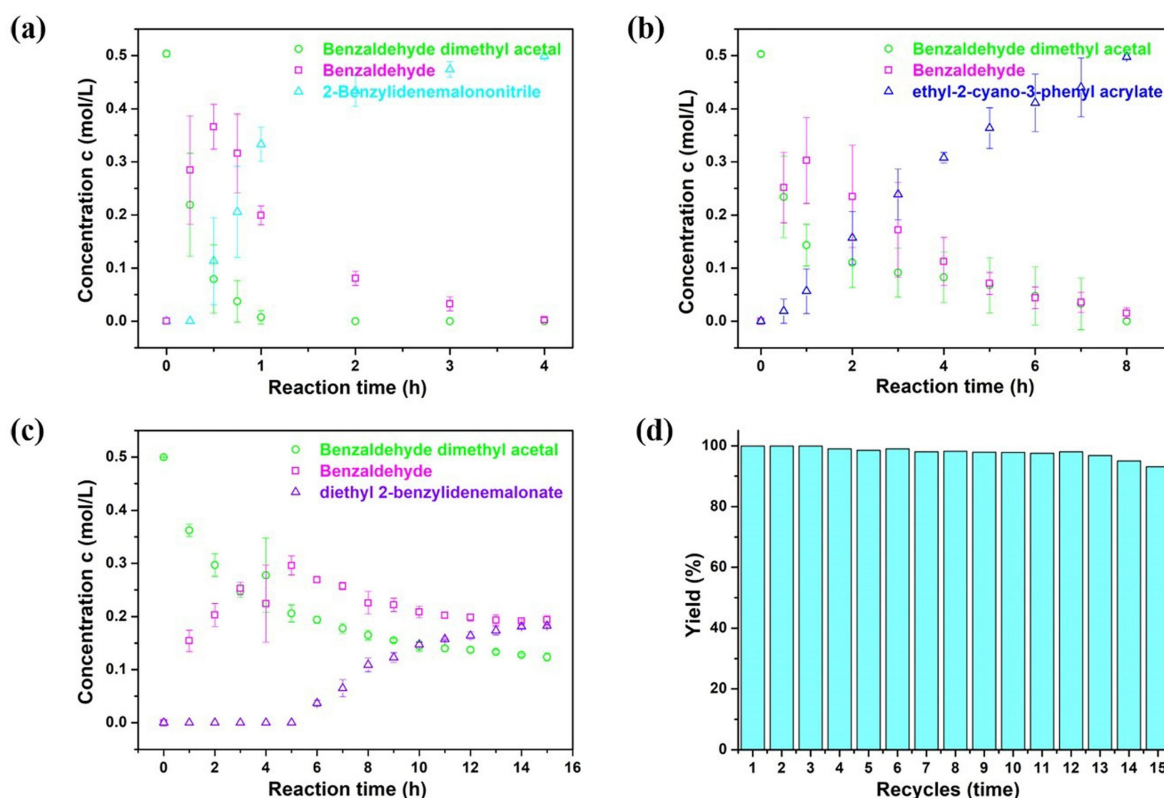


**Figure 4.** Acid (UiO-66-SO<sub>3</sub>H membrane) and base (UiO-66-NH<sub>2</sub> membrane) catalyzed reactions: a) from benzaldehyde dimethyl acetal to 2-benzylidene malononitrile in one-pot; b) from benzaldehyde dimethyl acetal to ethyl-2-cyano-3-phenyl acrylate in one-pot; c) from benzaldehyde dimethyl acetal to diethyl 2-benzylidene malonate in one-pot. d) Catalyst recycling studies. Reaction conditions: (2.5 mmol) dimethoxybenzyl acetal, (3 mmol) malononitrile, 50 mg UiO-66-SO<sub>3</sub>H membrane and 50 mg UiO-66-NH<sub>2</sub> membrane, solvent: DMF (5 mL), 80 °C.

experiments (without a catalyst) of the tandem reaction of benzaldehyde dimethyl acetal with different active methylene compounds (Table S4). Without the catalyst, the products 2-benzylidene malononitrile, ethyl-2-cyano-3-phenyl acrylate, and diethyl 2-benzylidene malonate were not detected in the one-pot two-step reactions. It indicated that the addition of the catalyst played an important role in the reaction process.

Next, we tested the recycling ability of the UiO-66-SO<sub>3</sub>H/-NH<sub>2</sub> membranes for the one-pot, two-step reaction of benzaldehyde dimethyl acetal with malononitrile. After the reaction is completed, the catalyst membranes only need to be simply taken out, washed with acetone and methanol, and dried in a vacuum oven at 80 °C. After this, it was directly used for the next catalytic cycles under the same reaction conditions. The results are shown in Figure 4d. When the catalyst membranes are reused 15 times, 2-benzylidene malononitrile can still be obtained as high as 93.1%. We carried out XRD characterization on the used catalyst membranes, as shown in Figure S4a, by comparison, there is no obvious difference between the used catalyst membranes and the fresh catalyst membranes, indicating that the catalyst membranes have good chemical resistance. In addition, we conducted Fourier-transform infrared (FT-IR) tests on the used catalyst membranes, as shown in Figure S4b, and the catalyst membranes can still maintain their integrity after 15 cycles of use. The performance of self-standing MOF membranes in one-pot reactions is compared with bifunctional acid-base MOF powders reported in the literature (Table S5). It can be seen that the self-supporting MOF membranes (UiO-66-SO<sub>3</sub>H/-NH<sub>2</sub> membranes) exhibit excellent catalytic activity and efficient recycling performance. As there was no change in the structure and physical integrity of the MOF membranes, they are expected to work for many more cycles, not limited to the 15 cycles as tested in this work.

## Conclusions

In conclusion, we present highly stable, easy-to-handle, reusable, efficient functional MOF self-standing membranes (UiO-66-SO<sub>3</sub>H and UiO-66-NH<sub>2</sub> membranes) for sustainable use as Wolf-Lamb-type (acid-base) catalysts in one-pot cascade reactions in a tea-bag-type concept. First, a simple procedure for making UiO-66-SO<sub>3</sub>H and UiO-66-NH<sub>2</sub> membranes based on in-situ growth of respective MOFs on seeded template polymer fibers in a non-woven is established. The membranes were characterized using routine analytical methods for porosity, morphology, and functionality and showed morphologically made up of hollow fibers. The membranes efficiently catalyzed both steps of a cascade one-pot reaction, i.e., deacetylation of benzaldehyde dimethyl acetal to benzaldehyde and reaction of active methylene compounds malononitrile and ethyl cyanoacetate with benzaldehyde. A high overall yield of the final products could be obtained. MOF membranes with -NH<sub>2</sub> base groups are limited as catalysts for the reaction of benzaldehyde with active methylene compounds having high pK<sub>a</sub>, such as diethyl malonate.

The membranes are easy to use and, after completion of the reaction, can be pulled out, washed, and reused without any significant drop in reaction efficiency, even after 15 cycles. This work provides an important step forward in preparing and using MOF membranes of macroscopic dimensions as sustainable catalysts.

## Experimental Section

### Materials

Zirconium(IV) chloride (ZrCl<sub>4</sub>, Alfa Aesar company, 99.5%), 2-aminobenzenedicarboxylic acid (BDC-NH<sub>2</sub>, Alfa Aesar company, 99%), 2-sulfobenzenedicarboxylic acid monosodium salt (BDC-SO<sub>3</sub>Na, Sigma Aldrich company), polyacrylonitrile (Mw = 80,000, Carl Roth), benzaldehyde dimethyl acetal (Alfa Aesar company, 99%), benzaldehyde (Alfa Aesar company, 99%), ethyl cyanoformate (Sigma Aldrich company, >99%), malononitrile (Alfa Aesar company, 99.5+%), diethyl malonate (Acros Organics company, >99%), Dodecane (Alfa Aesar company, 99%), acetic acid (Fisher Chemical Company, 99.7%), N, N-dimethylformamide (Fisher Chemical company, 99.5%) were purchased as stated.

### Preparation of UiO-66-SO<sub>3</sub>H particles and UiO-66-NH<sub>2</sub> particles

The solvothermal reaction was used to synthesize UiO-66-SO<sub>3</sub>H particles. 0.233 g ZrCl<sub>4</sub> and 0.268 g 2-sulfobenzenedicarboxylic acid monosodium salt (BDC-SO<sub>3</sub>Na) dissolved in 10 mL DI water and 1 mL acetic acid. Afterward, the mixture was transferred to a 50 mL Teflon-lined autoclave and reacted in an oven at 120 °C for 24 h. After cooling to room temperature, the white powder could be obtained by centrifugation and washing with 20 mL methanol 3–4 times, and finally dried at 100 °C overnight in an oven. The UiO-66-NH<sub>2</sub> particles are also synthesized by the solvothermal method. Just use 2-aminobenzenedicarboxylic acid instead of 2-sulfobenzenedicarboxylic acid monosodium salt (BDC-SO<sub>3</sub>Na). Other conditions are the same as synthetic UiO-66-SO<sub>3</sub>H particles.

### Preparation of UiO-66-SO<sub>3</sub>H membrane and UiO-66-NH<sub>2</sub> membrane

First, 0.33 g of ZrCl<sub>4</sub> and 1.0 g PAN were stirred in 5.6 g of DMF in 10 mL glass bottle for 3 h. The solution was used for electrospinning with an applied voltage 18.0 kV, flow rate 1.5 mL · h<sup>-1</sup>, and a 20.0 cm distance between the electrodes. This results in a PAN/ZrCl<sub>4</sub> fiber membrane. Next, 0.115 g ZrCl<sub>4</sub> and 0.134 g 2-sulfobenzenedicarboxylic acid monosodium salt (BDC-SO<sub>3</sub>Na) dissolved in 10 mL DI water and 1 mL acetic acid in 50 mL Teflon-lined autoclave. And then, 25 mg PAN/ZrCl<sub>4</sub> fiber membrane was added. The reaction was carried out in an oven at 120 °C for one day resulting in PAN/UiO-66-SO<sub>3</sub>H fiber membranes. Finally, the PAN was removed from the membranes by Soxhlet extraction at 165 °C for one day with DMF. The resulting UiO-66-SO<sub>3</sub>H fiber membrane free of PAN were dried. The preparation of the UiO-66-NH<sub>2</sub> membrane is the same as the UiO-66-SO<sub>3</sub>H fiber membrane. Use 2-aminobenzenedicarboxylic acid (BDC-NH<sub>2</sub>) instead of 2-sulfobenzenedicarboxylic acid monosodium salt (BDC-SO<sub>3</sub>Na).

The amount of acid and base groups were calculated based on the elemental analysis.

For UiO-66-SO<sub>3</sub>H membrane:

Elemental analysis: C 27.28%, H 3.63%, S 3.73%.

The amount of S =  $3.73/(32 \times 100) = 0.0011625$  mol/g of UiO-66-SO<sub>3</sub>H membrane = amount of acid group =  $0.58 \times 10^{-4}$  mol/50 mg membrane.

For UiO-66-NH<sub>2</sub> membrane:

Elemental analysis: C 34.26%, H 4.14%, N 3.96%.

The amount of N =  $3.96/(14 \times 100) = 0.002828$  mol/g of UiO-66-NH<sub>2</sub> membrane =

the amount of base groups (–NH<sub>2</sub>) =  $1.41 \times 10^{-4}$  mol/50 mg membrane.

## Catalytic experiment

### One-step acid-catalyzed reaction

Before catalyzing the reaction, the catalyst was activated in an oven at 353 K for 12 h to remove the solvent molecules. The reaction is carried out in the liquid phase under air. Typically, 2.5 mmol benzaldehyde dimethyl acetal, 5 mmol distilled water, 50 mg UiO-66-SO<sub>3</sub>H membrane, 0.75 mmol dodecane (as an internal standard), and 5 mL DMF were taken in a 25 mL glass reactor vial. The reaction mixture was then heated to 80 °C with stirring at 200 rpm. At regular intervals, 10 μL of the reaction mixture was taken using a pipette and the progress of the reaction was monitored by the GC-FID system (GC-2010 Plus, Shimadzu). After the reaction, the membrane is directly taken out of the reaction medium, washed with acetone (3 × 20 mL) and methanol (3 × 20 mL), dried at 80 °C in a vacuum oven, and reused for recycle runs.

### One-step base-catalyzed reaction

Before catalyzing the reaction, the catalyst was activated in an oven at 353 K for 12 h to remove the solvent molecules. The reaction is carried out in the liquid phase under air. 2.5 mmol benzaldehyde, 3 mmol active methylene compounds, 50 mg UiO-66-NH<sub>2</sub> membrane, 0.75 mmol dodecane (as an internal standard), and 5 mL DMF were taken in a 25 mL glass reactor vial. The reaction mixture was then heated to 80 °C with stirring at 200 rpm. At regular intervals, 10 μL of the reaction mixture was taken using a pipette and the progress of the reaction was monitored by GC-FID system (GC-2010 Plus, Shimadzu). After the reaction, the membrane is directly taken out of the reaction medium, washed with acetone (3 × 20 mL) and methanol (3 × 20 mL), dried at 80 °C in a vacuum oven, and reused for recycle runs.

### One-pot two-step acid-base catalyzed reaction

Before catalyzing the reaction, the catalyst was activated in an oven at 353 K for 12 h to remove the solvent molecules. The reaction is carried out in the liquid phase under air. Typically, 2.5 mmol benzaldehyde dimethyl acetal, 5 mmol distilled water, 3 mmol active methylene compounds, 50 mg UiO-66-SO<sub>3</sub>H membrane and 50 mg UiO-66-NH<sub>2</sub> membrane, 0.75 mmol dodecane (as an internal standard), and 5 mL DMF were taken in a 25 mL glass reactor vial. The reaction mixture was then heated to 80 °C with stirring at 200 rpm. At regular intervals, 10 μL of the reaction mixture was taken using a pipette and the progress of the reaction was monitored by GC-FID system (GC-2010 Plus, Shimadzu). After the reaction, the membranes are directly taken out of the reaction medium, washed with acetone (3 × 20 mL) and methanol (3 × 20 mL), dried at 80 °C in a vacuum oven, and reused for recycle runs.

## Acknowledgements

China Scholarship Council (CSC) is acknowledged for supporting the research stay of Yingying Du in the working group of Prof. Seema Agarwal. Open Access funding enabled and organized by Projekt DEAL.

## Conflict of Interest

The authors declare no conflict of interest.

## Data Availability Statement

The data that support the findings of this study are available in the supplementary material of this article.

**Keywords:** Metal-Organic Framework · electrospinning · cascade reactions

- [1] a) H. Demir, G. O. Aksu, H. C. Gulbalkan, S. Keskin, *Carbon Capture Science & Technology* **2022**, 2, 100026; *Technology* **2022**, 2, 100026; b) Y. Deng, Yanni. Wu, G. Chen, X. Zheng, M. Daia, C. Peng, *Chem. Eng. J.* **2021**, 405, 127004.
- [2] O. M. Yaghi, G. Li, H. Li, *Nature* **1995**, 378(6558), 703.
- [3] a) Y. Y. Liu, E. P. Hu, E. A. Khan, Z. P. Lai, *J. Membr. Sci.* **2010**, 353, 36; b) A. Huang, H. Bux, F. Steinbach, J. Caro, *Angew. Chem.* **2010**, 122, 5078.
- [4] X. Qin, Y. X. Sun, N. X. Wang, Y. B. Xie, J. R. Li, *Chem. Ind. Eng.* **2017**, 36, 1306.
- [5] L. Fan, M. Xue, Z. Kang, S. Qiu, *J. Mater. Chem.* **2012**, 22, 25272.
- [6] T. Toyao, M. Saito, Y. Horiuchi, M. Matsuoka, *Cata. Sci. Technol.* **2014**, 4, 625.
- [7] a) Y. Huang, A. M. Walji, C. H. Larsen, D. W. C. MacMillan, *J. Am. Chem. Soc.* **2005**, 127, 43, 15051; b) J. Barluenga, F. Rodríguez, F. J. Fanañus, *Chem. Asian J.* **2009**, 4, 1036; c) P. F. Xu, W. Wang, in *Catalytic cascade reactions*, John Wiley & Sons, **2013**; d) A. Behr, A. J. Vorholt, K. A. Ostrowski, T. Seidensticker, *Green Chem.* **2014**, 16, 982; e) Q. J. Liang, Y. H. Xu, T. P. Loh, *Org. Chem. Front.* **2018**, 5, 2765; f) H. Pellissier, *Adv. Synth. Catal.* **2020**, 362, 2289.
- [8] a) L. F. Tietze, *Chem. Rev.* **1996**, 96, 115; b) I. R. Baxendale, S. V. Ley, C. Piutti, *Angew. Chem.* **2002**, 114, Nr. 12; c) M. J. Climent, A. Corma, S. Iborra, *ChemSusChem* **2009**, 2, 500; d) C. Grondal, M. Jeanty, D. Enders, *Nat. Chem.* **2010**, 2, 167; e) A. Belluati, I. Craciun, J. Liu, C. G. Palivan, *Biomacromolecules* **2018**, 19, 4023; f) Y. Liu, J. A. Izzo, D. McLeod, S. Ričko, E. B. Svenningsen, T. B. Poulsen, K. A. Jørgensen, *J. Am. Chem. Soc.* **2021**, 143, 8208; g) W. Xu, L. Jiao, Y. Wu, L. Hu, W. Gu, C. Zhu, *Adv. Mater.* **2021**, 33, 2005172.
- [9] B. J. Cohen, M. A. Kraus, A. Patchornik, *J. Am. Chem. Soc.* **1981**, 103, 7621.
- [10] a) N. T. S. Phan, C. S. Gill, J. V. Nguyen, Z. J. Zhang, C. W. Jones, *Angew. Chem. Int. Ed.* **2006**, 45, 2209; b) J. P. H. Li, A. A. Adesina, E. M. Kennedy, M. Stockenhuber, *Phys. Chem. Phys.* **2017**, 19, 26630; c) X. Yuan, Z. Wang, Q. Zhang, J. Luo, *RSC Adv.* **2019**, 9, 23614.
- [11] a) K. Motokura, N. Fujita, K. Mori, T. Mizugaki, K. Ebitani, K. Kaneda, *J. Am. Chem. Soc.* **2005**, 127, 9674; b) A. Erigoni, M. C. Hernández-Soto, F. Rey, C. Segarra, U. Díaz, *Catal. Today* **2020**, 345, 227.
- [12] a) T. Ge, Z. Hua, Y. Zhu, Y. Song, G. Tao, X. Zhou, L. Chen, W. Ren, H. Yao, J. Shi, *RSC Adv.* **2014**, 4, 64871; b) K. A. Almeida, D. Cardoso, *Catal. Today* **2013**, 213, 122; c) A. Kawano, T. Moteki, M. Ogura, *Microporous Mesoporous Mater.* **2020**, 299, 110104.
- [13] a) M. Mu, X. Yan, Y. Li, L. Chen, *J. Nanopart. Res.* **2017**, 19, 148; b) J. H. Zhao, Y. Yang, J. X. Che, J. Zuo, X. H. Li, Y. Z. Hu, X. W. Dong, L. Gao, X. Y. Liu, *Chem. Eur. J.* **2018**, 24, 9903; c) S. Mistry, A. Sarkar, S. Natarajan, *Cryst. Growth Des.* **2019**, 19, 747; d) T. Zurrer, K. Wong, J. Horlyck, E. C.



- Lovell, J. Wright, N. M. Bedford, Z. Han, K. Liang, J. Scott, R. Amal, *Adv. Funct. Mater.* **2021**, *31*, 2007624.
- [14] a) Y. B. Huang, J. Liang, X. S. Wang, R. Cao, *Chem. Soc. Rev.* **2017**, *46*, 126; b) A. Dhakshinamoorthy, Z. Li, H. Garcia, *Chem. Soc. Rev.* **2018**, *47*, 8134; c) X. Zhang, J. Sun, G. Wei, Z. Liu, H. Yang, K. Wang, H. Fei, *Angew. Chem. Int. Ed.* **2019**, *58*, 2844; d) S. Yuan, J. Zhang, L. Hu, J. Li, S. Li, Y. Gao, Q. Zhang, L. Gu, W. Yang, X. Feng, B. Wang, *Angew. Chem.* **2021**, *133*, 21853; e) W. Yang, X. Liu, X. Chen, Y. Cao, S. Cui, L. Jiao, C. Wu, C. Chen, D. Fu, I. D. Gates, Z. Cao, H. Jiang, *Adv. Mater.* **2022**, 2110123.
- [15] a) P. Rani, R. Srivastava, *J. Colloid Interface Sci.* **2019**, *557*, 144; b) Y. Hu, J. Zhang, H. Huo, Z. Wang, X. Xu, Y. Yang, K. Lin, R. Fan, *Catal. Sci. Technol.* **2020**, *10*, 315; c) Y. R. Lee, X. H. Do, S. S. Hwang, K. Y. Baek, *Catal. Today* **2021**, *359*, 124.
- [16] Q. Dang, H. Huang, L. Li, X. Lyu, S. Zhong, Y. Yu, D. Xu, *Chem. Mater.* **2021**, *33*, 5690.
- [17] J. Liu, T. A. Goetjen, Q. Wang, J. G. Knapp, M. C. Wasson, Y. Yang, Z. H. Syed, M. Delferro, J. M. Notestein, O. K. Farha, J. T. Hupp, *Chem. Soc. Rev.* **2022**, *51*, 1045.
- [18] F. Mitschang, H. Schmalz, S. Agarwal, A. Greiner, *Angew. Chem. Int. Ed.* **2014**, *53*, 4972.
- [19] M. O. Pletscher, S. Gekle, S. Agarwal, *Macromol. Rapid Commun.* **2019**, *40*, 1900148.
- [20] J. H. Cavka, S. Jakobsen, U. Olsbye, N. Guillou, C. Lamberti, S. Bordiga, K. P. Lillerud, *J. Am. Chem. Soc.* **2008**, *130*, 13850.
- [21] M. J. Katz, Z. J. Brown, Y. J. Colón, P. W. Siu, K. A. Scheidt, R. Q. Snurr, J. T. Hupp, O. K. Farha, *Chem. Commun.* **2013**, *49*, 9449.
- [22] Y. Yang, H. F. Yao, F. G. Xi, E. Q. Gao, *J. Mol. Catal. A* **2014**, *390*, 198.
- [23] R. G. Vaghei, D. Azarifar, S. Daliran, A. R. Oveisi, *RSC Adv.* **2016**, *6*, 29182.
- [24] M. Thommes, K. Kaneko, A. V. Neimark, J. P. Olivier, F. Rodriguez-Reinoso, J. Rouquerol, K. S. W. Sing, *Pure Appl. Chem.* **2015**, *87*, 1051.
- [25] C. Schlumberger, M. Thommes, *Adv. Mater. Interfaces* **2021**, *8*, 2002181.
- [26] J. Rouquerol, F. Rouquerol, P. Llewellyn, G. Maurin, K. S. W. Sing, Academic press, **2013**.
- [27] W. S. Matthews, J. E. Bares, J. E. Bartmess, F. G. Bordwell, F. J. Cornforth, G. E. Drucker, Z. Margolin, R. J. McCallum, G. J. McCollum, N. R. Vanier, *J. Am. Chem. Soc.* **1975**, *97*, 7006.
- [28] a) D. Wang, Z. Li, *Catal. Sci. Technol.* **2015**, *5*, 1623; b) H. Liu, F. G. Xi, W. Sun, N. N. Yang, E. Q. Gao, *Inorg. Chem.* **2016**, *55*, 12, 5753.

---

Manuscript received: August 18, 2022  
Revised manuscript received: September 20, 2022  
Accepted manuscript online: October 2, 2022  
Version of record online: October 28, 2022